RSC Advances

ROYAL SOCIETY OF CHEMISTRY

www.rsc.org/advances

Table of Contents (TOC) Image

Capturing hepatocellular carcinoma cells using lactobionic acid-functionalized electrospun polyvinyl alcohol/polyethyleneimine nanofibers†

Yili Zhao,[1] Zhangyu Fan,[2] Mingwu Shen,[2] Xiangyang Shi*[1, 2]

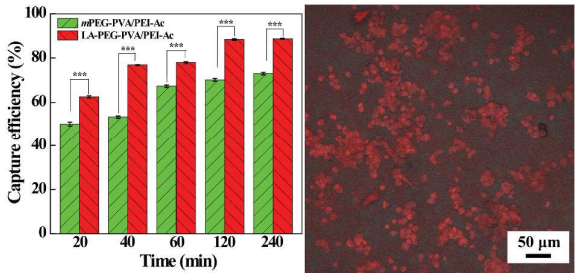

Crosslinked PVA/PEI nanofibers can be functionalized with lactobionic acid *via* a PEG spacer for specific capture of hepatocellular carcinoma cells.

Cite this: DOI: 10.1039/c0xx00000x

www.rsc.org/xxxxxx

PAPER

Capturing hepatocellular carcinoma cells using lactobionic acid-functionalized electrospun polyvinyl alcohol/polyethyleneimine nanofibers†

Yili Zhao,[a] Zhangyu Fan,[b] Mingwu Shen,[b] Xiangyang Shi*[a, b]

Received (in XXX, XXX) Xth XXXXXXXXX 20XX, Accepted Xth XXXXXXXXX 20XX
DOI: 10.1039/b000000x

We report a facile approach to immobilizing lactobionic acid (LA) onto electrospun polyvinyl alcohol (PVA)/polyethyleneimine (PEI) nanofibers through a polyethylene glycol (PEG) spacer for capturing hepatocellular carcinoma cells. In this work, electrospun PVA/PEI nanofibers were crosslinked using glutaraldehyde vapor, covalently conjugated with PEGylated LA *via* N-(3-dimethy-laminopropyl)-N'-ethylcarbodiimide hydrochloride (EDC) coupling reaction, followed by acetylation of the remaining PEI amines on the fiber surface. The formed LA-functionalized nanofibers were characterized *via* scanning electron microscopy and attenuated total reflectance-Fourier transform infrared spectroscopy. We show that the fiber morphology does not significantly change after the fiber surface modification. The functionalized nanofibers display good hemocompatibility and superior capability to capture asialoglycoprotein receptor (ASGPR)-overexpressing hepatocellular carcinoma cells *in vitro via* ligand-receptor interaction. The developed LA-modified PVA/PEI nanofibers may be applied to capture circulating tumor cells for cancer diagnosis applications.

Introduction

Hepatocellular carcinoma (HCC) is the third-leading cause of cancer-related mortality worldwide because of the high prevalence of its main etiological agents, chronic hepatitis B virus (HBV) and hepatitis C virus (HCV) infections.[1, 2] Therefore, early and accurate detection of HCC using advanced technologies is of paramount importance. One major strategy used to diagnose cancer cells is through the capture and detection of circulating tumor cells (CTCs) that can escape from primary tumor, shed into the vasculature and circulate in the bloodstream, eventually lead to the subsequent growth of additional tumors (metastasis) in vital distant organs.[3] It has been regarded that CTCs usually trigger a mechanism that is responsible for the vast majority of cancer-related deaths, thus capturing CTCs is essential for cancer diagnosis.[4]

Electrospinning has been recognized as a versatile and powerful technique to fabricate ultralong synthetic or natural polymer nanofibers with fiber diameter ranging from tens of nanometers to several micrometers.[5-8] The intriguing physicochemical properties of electrospun nanofibers such as extremely large surface area to volume ratio, high porosity, superior mechanical durability, similar dimensions to cellular surface components (e.g., microvilli and filopodia), and capability to mimic the extracellular matrix (ECM) enable them to be widely used in the fields of tissue engineering[9-13] and drug delivery.[14-17]

Recently, electrospun nanofibers have been employed as substrates to capture circulating tumor cells (CTCs). Prior to the capture of cancer cells, various specific biomarker molecules such as epithelial cell adhesion molecule antibody (anti-EpCAM),[18-23] aptamers,[24-27] polypeptide,[28, 29] or E-selectin[30] have been immobilized to induce specifically enhanced cell capture ability. For instance, Liu *et al.* fabricated MnO_2 nanofibers by a standard photolithography and an electrospinning process, followed by further modification of anti-EpCAM for capturing EpCAM-positive breast cancer cells.[31] In our previous study, we modified folic acid (FA)-functionalized dendrimers onto the surface of electrospun cellulose acetate nanofibers through a layer-by-layer assembly technique in combination with an N-(3-dimethy-laminopropyl)-N'-ethylcarbodiimide hydrochloride (EDC) coupling reaction in order to capture FA receptor-overexpressing cancer cells.[32] However, most of the studies require sophisticated biofunctionalization steps. It is desirable to seek a polymer system that can be easily electrospun to form nanofibers and possesses intrinsic reactive functional groups, allowing for easy modification of biological molecules onto the nanofiber surface to render the fibers with specific cancer cell capture ability.

Polyethylenimine (PEI) is a water-soluble aliphatic polyamine that contains abundant primary, secondary, and tertiary amines.[33, 34] Our previous work has shown that electrospun polyvinyl alcohol (PVA)/polyethyleneimine (PEI) nanofibers can be formed and rendered with water stability through glutaraldehyde (GA) vapor crosslinking.[35, 36] In addition, we have also shown that PEI-coated nanoparticles can be easily functionalized with different targeting ligands such as FA,[37] arginine-glycine-aspartic acid

(RGD) peptide,[38] and hyaluronic acid (HA)[39] through PEI amine-mediated coupling reaction.

Asialoglycoprotein receptors (ASGPR) overexpressed on the surface of HCC cells possess strong binding affinity with galactose, facilitating efficient intracellular uptake of the galactose ligands or the galactose ligand-modified conjugates.[40] As a kind of oligosaccharide aldonic acid containing carbohydrate (galactose) and aldonic acid (gluconic acid), lactobionic acid (LA) has been regarded as a useful ligand for specific targeting to HCC cells.[41, 42] For instance, LA-modified dendrimer-entrapped gold nanoparticles have been fabricated and used as a nanoprobe for specific computed tomography imaging of ASGPR-overexpressing HCC cells *in vitro* and the xenoplanted tumor model *in vivo*.[43, 44] In another study, laponite nanodisks have been conjugated with PEGylated LA for anticancer drug encapsulation and targeted delivery to HCC cells.[45] Therefore, it is reasonable to hypothesize that the PVA/PEI nanofibers functionalized with LA may be used to capture ASGPR-overexpressing HCC cells by virtue of the ECM-mimicking structure of the nanofibers and the high selectivity of LA moieties to recognize the HCC cells.

In this present study, we developed a convenient approach to immobilizing LA onto the GA vapor-crosslinked electrospun PVA/PEI nanofibers *via* a PEG spacer, followed by acetylation to neutralize the remaining PEI amines on the fiber surface (Scheme 1). The LA-functionalized nanofibers were characterized *via* scanning electron microscopy (SEM), attenuated total reflectance-Fourier transform infrared spectroscopy (ATR-FTIR), and tensile tests. The hemocompatibility of the fibers was assessed *via* hemolytic assay of human red blood cells (HRBCs) and the ability of the fibers to capture ASGPR-overexpressing HCC cells was investigated in detail. To our knowledge, this is the first report related to the use of LA-functionalized electrospun PVA/PEI nanofibers for specific HCC cell capture applications.

Experimental

Materials

Branched PEI (Mw = 25,000) with a concentration of 50% in aqueous solution, LA, and propidium iodide (PI) were obtained from Aldrich (St. Louis, MO). PVA (Mw = 88 000) hydrolyzed to an extent of 88% and EDC were purchased from J&K Chemical Ltd. (Beijing, China). N-hydroxysuccinimide (NHS) was from GL Biochem Ltd. (Shanghai, China). GA (25% in aqueous solution), triethylamine, and acetic anhydride were provided by Sinopharm Chemical Reagent Co., Ltd. (Shanghai, China). Both PEG monomethyl ether with carboxyl end group (*m*PEG-COOH, Mw = 2,000) and dual functional PEG (NH_2-PEG-COOH, Mw = 2,000) were purchased from Shanghai Yanyi Biotechnology Corporation (Shanghai, China). Regenerated cellulose dialysis membranes with a molecular weight cut-off (MWCO) of 500 were acquired from Fisher (Pittsburgh, PA). HepG2 cells (a human liver HCC cell line) and HeLa cells (a human cervical carcinoma cell line) were supplied by Institute of Biochemistry and Cell Biology (the Chinese Academy of Sciences, Shanghai, China). Modified Eagle Medium (MEM), Duibecco's Modified Eagle Medium (DMEM), fetal bovine serum (FBS), penicillin, and streptomycin were purchased from Hangzhou Jinuo Biomedical Technology (Hangzhou, China). All chemicals were used as received. Water used in all experiments was purified using a Milli-Q Plus 185 water purification system (Millipore, Bedford, MA) with a resistivity higher than 18.2 MΩ·cm.

Synthesis of LA-PEG-COOH conjugate

According to the procedure reported in the literatures,[43-45] LA was reacted with NH_2-PEG-COOH *via* an EDC/NHS coupling reaction to form the LA-PEG-COOH conjugate. In a typical procedure, a NaH_2PO_4-Na_2HPO_4 solution of EDC (0.15 mmol, 1 mL) and NHS (0.15 mmol, 1 mL) was sequentially added into a NaH_2PO_4-Na_2HPO_4 solution (pH = 6.0, 0.02 M, 5 mL) of LA (0.15 mmol). The mixture was then vigorously stirred for 3 h at room temperature to activate the carboxyl group of LA. Thereafter, the activated LA was added into a NaH_2PO_4-Na_2HPO_4 solution (pH = 6.0, 0.02 M, 7 mL) of NH_2-PEG-COOH (0.10 mmol) and continuously stirred for 3 days. Finally, the mixture was dialyzed against water using a dialysis membrane with an MWCO of 500 for 3 days, followed by lyophilization to form the LA-PEG-COOH conjugate. The conjugate was stored at -20 ºC before further use.

Preparation of water-stable PVA/PEI nanofibers

PVA/PEI at a weight ratio of 3:1 were dissolved into an aqueous solution at an optimized concentration of 12% according to protocols described in our previous studies.[35, 36] Briefly, PVA powder (9.69 g) was dissolved into water (71.04 g) at a temperature of 80 °C for 3 h under continuous stirring, then cooled down to room temperature, and stored at 4 ºC for future use. An aqueous PEI solution (0.6 g) and water (4.4 mL) were sequentially added into the above PVA solution (15 g) under magnetic stirring overnight until a clear and homogeneous solution was obtained. The PVA/PEI nanofibers were fabricated *via* a commercial electrospinning equipment (1006 Electrospinning Equipment, Beijing Kang Sente Technology Co., Ltd., Beijing, China) using a stainless needle with an inner diameter of 0.8 mm. A clamp was used to connect the high voltage power supply with the needle. A thin aluminum foil which acts as a collector was positioned vertically and grounded, and the tip-to-collector distance was set at 25 cm. During the electrospinning process, the voltage was fixed at 18.6 kV. The flow rate of the electrospinning solution was controlled by a syringe pump at 0.3 mL/h. The electrospinning equipment was maintained at a humidity of 40-50% and at 25 ºC. After electrospinning for 5 h, the nanofibrous mat was crosslinked by GA vapor in a vacuum desiccator for 18 h to render it water stable. Finally, the GA-crosslinked nanofibrous mat was peeled off from the collector and dried in vacuum at ambient temperature for at least 2 days to remove the residual GA and moisture.

Preparation of LA-functionalized PVA/PEI nanofibrous mat

PEGylated LA (LA-PEG-COOH) was modified onto the surface of the GA-crosslinked PVA/PEI nanofibrous mat by reacting with the PEI amines through an EDC/NHS coupling reaction. Briefly, an aqueous solution of EDC (0.31 mmol, 10 mL) and NHS (0.31 mmol, 10 mL) was sequentially added into an aqueous solution of the LA-PEG-COOH conjugate (0.062 mmol, 10 mL) under

vigorous stirring for 3 h to activate the carboxyl group of the LA-PEG-COOH conjugate. After that, a piece of GA-crosslinked PVA/PEI nanofibrous mat with a diameter of 12.5 cm (120.4 mg, with molar ratio between the total PEI primary and secondary amines and LA-PEG-COOH carboxyl group of 10:1) was immersed into the activated LA-PEG-COOH aqueous solution under gentle shaking at room temperature for 3 days. Then, triethylamine (391.82 μL, 2.815 mol) was added into the above suspension under gentle shaking for 30 min, followed by addition of acetic anhydride (266.10 μL, 2.815 mol) under gentle shaking for 24 h to neutralize the remaining PEI amines of the nanofibers. Finally, the nanofibrous mat (denoted as LA-PEG-PVA/PEI-Ac) was thoroughly washed with water and dried in vacuum before characterization and use. For comparison, *m*PEG-COOH was functionalized onto the GA-crosslinked PVA/PEI nanofibrous mat to prepare nontargeted PVA/PEI-Ac nanofibrous mat (denoted as *m*PEG-PVA/PEI-Ac) following the same experimental procedures.

Characterization techniques

^{1}H NMR spectrum of the LA-PEG-COOH conjugate was recorded using Bruker AV-400 NMR spectrometer (Mannheim, Germany). Samples were dissolved in D_2O at a concentration of 6.0 mg/mL before measurement. Morphologies of the PVA/PEI nanofibers, GA vapor-crosslinked PVA/PEI nanofibers, and *m*PEG-PVA/PEI-Ac or LA-PEG-PVA/PEI-Ac nanofibers were observed using SEM (JEOL JSM-5600LV, Tokyo, Japan) at an operation voltage of 10 kV. Before SEM observations, the samples were sputter coated with a gold film with a thickness of 10 nm. The fiber diameter distribution was measured using Image J 1.40G software (http://rsb.info.nih.gov/ij/down-load.html). For each sample, at least 300 nanofibers from different images were randomly selected and analyzed. ATR-FTIR was performed on a Nicolet Nexus 670 FTIR spectrometer (Thermo Nicolet Corp., Denver, CO) using a transmission mode in a wavenumber range of 400-4000 cm^{-1}. Mechanical properties of the GA vapor-crosslinked PVA/PEI, *m*PEG-PVA/PEI-Ac, and LA-PEG-PVA/PEI-Ac nanofibers were tested by a material testing machine (H5K-S, Hounsfield, UK) at constant temperature (20 °C) and humidity (63%) with a cross-head speed of 10 mm min^{-1} under a load of 10 N. The fiber samples were cut into rectangular pieces with width×length = 10 mm×50 mm. The thickness of the samples was measured with a micrometer. Then, the two ends of sample were gripped in the top and bottom chucks, respectively, and the gauge of two chucks connected to the testing machine was fixed at 30 mm. The stress and strain data were calculated using Equations 1 and 2:

$$\sigma(MPa) = \frac{P(N)}{w(mm) \times d(mm)} \quad (1)$$

$$\varepsilon = \frac{l}{l_0} \times 100\% \quad (2)$$

Where σ, ε, P, w, d, l, and l_0 stand for stress, strain, strength, width, thickness, extension length, and gauge length, respectively. Breaking strength, failure strain, and Young's modulus were obtained from the strain-stress curves. Mechanical property tests were done in triplicate and the results were reported as mean ± SD.

Hemolysis assay

Hemolysis assay was performed to evaluate the hemocompatibility of the nanofibrous mat. In brief, heparin stabilized fresh human blood provided by Shanghai General Hospital (Shanghai, China) was centrifuged (3000 rpm, 3 min), and the precipitate was washed with phosphate buffer saline (PBS) for 3 times to completely remove serum and obtain human red blood cells (HRBCs). Thereafter, the HRBCs were diluted 35-fold with PBS before hemolysis assay. The diluted HRBC suspension (0.2 mL) was mixed with a PBS solution (0.8 mL) in a 1.5-mL Eppendorf tube containing *m*PEG-PVA/PEI-Ac (2 mg) or LA-PEG-PVA/PEI-Ac nanofibers (2 mg). Diluted HRBCs (0.2 mL) mixed with 0.8 mL water (as positive control) or 0.8 mL PBS (as negative control) were also tested for comparison. After gentle shaking, all samples were incubated at 37 °C for 2 h, followed by centrifugation at 10,000 rpm for 1 min. The photo of the samples was taken and the absorbance of the supernatants (hemoglobin) was recorded using a Lambda 25 UV-vis spectrophotometer (Perkin Elmer, Boston, MA) with a wavelength range of 450-800 nm. The hemolytic percentage (HP) was calculated by dividing the difference of the absorbance at 540 nm between the test sample and the negative control by the difference of the absorbance at 540 nm between the positive and the negative control. Under the same conditions, the hemocompatibility of unmodified GA vapor-crosslinked PVA/PEI nanofibers was also tested.

Cell culture

HepG2 cells with high ASGPR expression or HeLa cells without ASGPR expression[46, 47] were continuously cultured in 25 cm^2 tissue culture flasks with 5 mL of MEM or DMEM supplemented with 10% FBS, 100 U/mL penicillin, and 100 μg/mL streptomycin in a humidified incubator with 5% CO_2 at 37 °C.

Specific cell capture assay

For specific capture of ASGPR-overexpressing HCC cells, the *m*PEG-PVA/PEI-Ac or LA-PEG-PVA/PEI-Ac nanofibrous mats with a circular shape (diameter = 14 mm) in quadruplicate were fixed in a 24-well tissue culture plate (TCP) using stainless steel rings and sterilized by exposure to 75% alcohol solution under ultraviolet light for 2 h. After that, the samples were washed 3 times with PBS and soaked in MEM overnight before cell seeding. Then, 1×10^5 HepG2 cells in 400 μL medium were seeded into each well. After incubation in a humidified incubator with 5% CO_2 and 95 % relative humidity at 37 ºC for 10, 20, 40, 60, 120 and 240 min, respectively, the medium was gently shaken and transferred to a 15-mL centrifuge tube, and the nanofibrous mats were gently washed 3 times with PBS in order to collect all the HepG2 cells that were not captured by the nanofibrous mats. After mixing the collected cell suspension and PBS washing solution, the number of unattached HepG2 cells was counted using a Scepter 2.0 Handheld Automated Cell Counter (Merck Millipore, Merck KGaA, Damstadt, Germany). The number of captured cells can be deduced from the difference of the initial seeding cells and the unattached cells. The cell capture efficiency was calculated by dividing the number of captured cells by that of the initial seeding cells. For comparison, the unmodified crosslinked PVA/PEI nanofibers were also used to capture

HepG2 cells under the same conditions.

To further prove the targeted cancer cell capture ability of the *m*PEG-PVA/PEI-Ac and LA-PEG-PVA/PEI-Ac nanofibrous mats, HeLa cells without ASGPR expression were also seeded onto the fiber surface, treated, and the cell capture efficiency was calculated using the same method.

Confocal microscopy

Beside the quantitative analysis, the cell capture capacity was also qualitatively evaluated *via* confocal microscopic observation of the nanofibrous mats with the captured cells. Electrospun PVA/PEI nanofibers were directly formed onto the surface of cover slips, followed by modification with PEGylated LA and acetylation of the remaining PEI amines according to the above conditions. HeLa cells at a density of 1×10^5 cells per well were cultured onto both the *m*PEG-PVA/PEI-Ac and LA-PEG-PVA/PEI-Ac nanofibrous mats for 10, 20, 40, 60, 120, and 240 min, respectively. Thereafter, the nanofibrous mats were gently washed 3 times with PBS, fixed with 2.5 wt% GA at 4 °C for 30 min, and stained with PI (1 mg/mL, 20 μL) at 37 °C for 15 min, followed by washing with PBS. The samples were imaged using confocal microscopy (Carl Zeiss LSM 700, Jena, Germany) *via* a 10× objective lens.

SEM observation of cancer cells captured by the fibrous mats

The morphology of the HepG2 cells captured onto the *m*PEG-PVA/PEI-Ac or LA-PEG-PVA/PEI-Ac nanofibrous mats was also observed by SEM. After HepG2 cells were cultured onto the nanofibrous mats for 240 min, each sample was rinsed 3 times with PBS and fixed with 2.5% GA for 2 h at 4 °C, followed by dehydration with a series of gradient ethanol solutions (50%, 70%, 80%, 90%, and 100% ethanol, respectively) and air-dried. Then the samples were sputter coated with 10 nm thick gold film and observed by SEM at an operating voltage of 10 kV.

Statistical analysis

Statistical analysis was performed by one-way ANOVA method to evaluate the significance of the experimental data. In all evaluations, 0.05 was selected as the significance level, and the data were indicated with (*) for $p < 0.05$, (**) for $p < 0.01$, and (***) for $p < 0.001$, respectively.

Results and discussion

Synthesis of the LA-PEG-COOH conjugate

^{1}H NMR was used to characterize the synthesized LA-PEG-COOH conjugate (Figure 1). The peak at 3.5 ppm can be assigned to the PEG -CH_2- protons, and the characteristic proton peaks at 3.4 to 4.3 ppm are associated to the LA moieties, confirming the successful PEGylation of LA, in agreement with our previous reports.[43, 44] Based on NMR peak integration associated to the NH_2-PEG-COOH and the LA, the number of LA moieties attached to each NH_2-PEG-COOH was estimated to be 1.0.

Fabrication of water-stable electrospun PVA/PEI nanofibers

SEM was used to observe the morphology of the electrospun PVA/PEI nanofibers before and after crosslinking (Figure 2). Clearly, under the optimized electrospinning conditions reported in our previous work,[35, 36] uniform and smooth PVA/PEI nanofibers with random orientation are formed with a mean fiber diameter of 439 ± 62.9 nm (Figure 2a). After GA vapor crosslinking, the porous structure of the nanofibrous mat is still well maintained and the fiber diameter is slightly increased to 525 ± 69.6 nm (Figure 2b), which is likely due to the swelling of the PVA/PEI nanofibers during the crosslinking process. In addition, the white color of the pristine PVA/PEI nanofibrous mat changed to yellowish after crosslinking, suggesting the successful crosslinking reaction, in agreement with the literature.[48]

ATR-FTIR spectroscopy was then carried out to further characterize the GA vapor-crosslinked PVA/PEI nanofibers (Figure 3). The peaks at 3350 cm^{-1} and 2940 cm^{-1} belong to the O-H and the -CH_2- stretching vibrations, respectively (Curve 1). Compared with the pristine PVA/PEI nanofibers before crosslinking, the N-H bending of the primary amines of PEI at 1700 cm^{-1} still exists after GA vapor crosslinking, suggesting that the PEI primary amines are available for further modification. However, the N-H outer bending vibration at 918 cm^{-1} becomes weak after the crosslinking reaction. In addition, a new peak at 1650 cm^{-1} representing the formation of aldimine linkage between the PEI amines and GA emerges, indicating the successful crosslinking reaction, in agreement with our previous work.[35, 36, 49]

Modification of LA-PEG-COOH onto PVA/PEI nanofibrous mat

The GA vapor-crosslinked PVA/PEI nanofibrous mat was then modified with LA-PEG-COOH through an EDC/NHS coupling reaction, followed by acetylation of the remaining PEI surface amines (Scheme 1). As can be seen from the SEM images (Figure 4), the formed *m*PEG-PVA/PEI-Ac and LA-PEG-PVA/PEI-Ac nanofibers still maintain a smooth and uniform fibrous morphology, except that the fiber diameter increases to 509 ± 81.7 nm and 579 ± 74.5 nm when compared to that of the crosslinked PVA/PEI nanofibers before LA modification, which is presumably due to the swelling during the GA vapor crosslinking and the PEGylation modification process in aqueous solution.

The formed *m*PEG-PVA/PEI-Ac and LA-PEG-PVA/PEI-Ac nanofibers were also characterized by ATR-FTIR spectroscopy (Figure 3). It can be seen that the amide I stretching bands at 1610 cm^{-1} increases for both the *m*PEG-PVA/PEI-Ac and LA-PEG-PVA/PEI-Ac nanofibers, indicating the successful reaction between the carboxyl groups of LA-PEG-COOH or *m*PEG-COOH and the PEI amines on the fiber surface. In addition, the N-H bending intensity of the PEI primary amines at 1700 cm^{-1} decreases, suggesting the successful acetylation of the PEI amines on the surface of the nanofibers. Overall, ATR-FTIR qualitatively confirmed the successful fiber surface modification.

The mechanical property of the GA vapor-crosslinked PVA/PEI, *m*PEG-PVA/PEI-Ac, and LA-PEG-PVA/PEI-Ac nanofibers was also tested (Table 1 and Figure 5). The breaking strength, failure strain, and Young's modulus of either *m*PEG-PVA/PEI-Ac or LA-PEG-PVA/PEI-Ac nanofibers are much larger than those of the unmodified GA vapor-crosslinked PVA/PEI nanofibers. This is likely due to the fact that the modification of *m*PEG or LA-PEG onto the fiber surfaces leads to enhanced solidification or fixation of the single fibers. The failure

strain of the LA-PEG-PVA/PEI-Ac nanofibers is slightly higher than that of the *m*PEG-PVA/PEI-Ac nanofibers, whereas their breaking strength and Young's modulus are lower, suggesting that the mechanical property of the fibrous materials is also slightly dependent on the type of the modified molecules.

Hemocompatibility assay

Hemocompatibility of the formed *m*PEG-PVA/PEI-Ac or LA-PEG-PVA/PEI-Ac nanofibrous mats is of paramount importance for capturing cancer cells circulating in the blood. A hemolytic assay was employed to evaluate the hemocompatibility of the fibrous mats (Figure 6). In contrast to the positive control, where HRBCs exposed to water are totally damaged (inset of Figure 6a, vial 1), HRBCs treated with the *m*PEG-PVA/PEI-Ac or LA-PEG-PVA/PEI-Ac nanofibrous mats do not show any obvious hemolytic effect (inset of Figure 6a, vial 3 and 4), similar to the negative PBS control (inset of Figure 6a, vial 2). The hemolytic effect of each material was further quantified based on the absorbance of the hemoglobin released from the lysed HRBCs at 540 nm. The hemolysis percentages of the *m*PEG-PVA/PEI-Ac and LA-PEG-PVA/PEI-Ac nanofibrous mats were measured to be 1.66% and 3.94%, respectively, much lower than the threshold value of 5%,[50] indicating the good hemocompatibility of both nanofibers. Similarly, the unmodified GA vapor-crosslinked PVA/PEI nanofibrous mats display a hemolysis percentage of 2.87%, also showing no hemolytic effect (Figure S1, Electronic Supplementary Information, ESI).

Cell capture assay

To confirm the specific cancer cell capturing ability of the formed LA-PEG-PVA/PEI-Ac nanofibrous mat, ASGPR-overexpressing HepG2 cells were cultured using the LA-PEG-PVA/PEI-Ac nanofibrous mat as substrate. *m*PEG-PVA/PEI-Ac nanofibrous mat without LA was used as control. As shown in Figure 7a, the HepG2 cell capture efficiency of the *m*PEG-PVA/PEI-Ac and the LA-PEG-PVA/PEI-Ac nanofibrous mats increases with the incubation time. At a given time point, the HepG2 cell capture efficiency of the LA-PEG-PVA/PEI-Ac nanofibrous mat is significantly higher than that of the *m*PEG-PVA/PEI-Ac nanofibrous mat ($p < 0.001$). This suggest that the LA-modification onto the nanofibers is able to greatly enhance the capture ability of the fibrous mat presumably through the specific targeting of LA to ASGPR-overexpressing HCC cells. It is also noted that the efficiency of unmodified crosslinked PVA/PEI nanofibrous mats to capture HepG2 cells increases with the incubation time (Figure S2, ESI), and at 240 min, the cell capture efficiency reaches 70.37%, which is quite similar to that of the *m*PEG-PVA/PEI-Ac nanofibrous mat (73.06%). In contrast, for HeLa cells without ASGPR expression, almost the same capture efficiency can be achieved by the *m*PEG-PVA/PEI-Ac and the LA-PEG-PVA/PEI-Ac nanofibrous mat at the same time point (Figure 7b). For both cells with or without ASGPR expression, the increased cell capture efficiency with the incubation time for both the *m*PEG-PVA/PEI-Ac and the LA-PEG-PVA/PEI-Ac nanofibrous mat should be due to the nonspecific adhesion of cells onto the surface of nanofibers with a porous ECM-mimicking topographic structure.

Further qualitative confocal microscopic observation reveals that much more HepG2 cells (stained in red) are able to be captured by the LA-PEG-PVA/PEI-Ac nanofibrous mat than by the *m*PEG-PVA/PEI-Ac mat without LA (Figure 8) at the same time point. The confocal microscopy data further validate the quantitative cell capture assay.

To clearly reveal the morphology of the captured cells on the surface of the *m*PEG-PVA/PEI-Ac or LA-PEG-PVA/PEI-Ac nanofibers, SEM was performed (Figure 9). It can be seen that cells attached onto the LA-PEG-PVA/PEI-Ac nanofibrous mat exhibit long filopodia and have a relatively large contact area with the fibers (Figures 9c and 9d), whereas cells captured onto the *m*PEG-PVA/PEI-Ac nanofibrous mat display a round shape and are quite isolated (Figures 9a and 9b). This further indicates the role of the modified LA to enhance the cell capture *via* ligand-receptor interaction. Apparently, the number of cells captured by the LA-PEG-PVA/PEI-Ac nanofibrous mat is much larger than that by the *m*PEG-PVA/PEI-Ac nanofibers, corroborating the confocal microscopic observation. Taken together, our results clearly indicate that LA-PEG-PVA/PEI-Ac nanofibrous mat is able to specifically capture ASGPR-overexpressing HepG2 cells *via* the LA-mediated specific ligand-receptor interaction.

Conclusion

In summary, we present a facile approach to modifying LA onto crosslinked PVA/PEI nanofibrous mat *via* a PEG spacer to render it with specific capture capacity of HCC cells. The modification of PEGylated LA onto the nanofiber surface does not compromise the smooth and uniform morphology of the nanofibers. The formed LA-functionalized PVA/PEI nanofibrous mat displays enhanced mechanical durability, good hemocompatibility and ability to capture ASGPR-overexpressing HCC cells with high specificity. The developed LA-functionalized PVA/PEI nanofibrous mat with the ECM-mimicking nanofibrous structure may be potentially used to capture HCC cells circulating in blood for monitoring the stage of metastasis.

Acknowledgements

This research is financially supported by the Program for Professor of Special Appointment (Eastern Scholar) at Shanghai Institutions of Higher Learning and the Key Laboratory of Textile Science & Technology, Ministry of Education, "111 Project", B07024. M. Shen thanks the Fundamental Research Funds for the Central Universities. Y. Zhao thanks the Chinese Universities Scientific Fund (101-06-0019014).

Notes and references

[a] *Key Laboratory of Textile Science & Technology, Ministry of Education, College of Textiles, Donghua University, Shanghai 201620, People's Republic of China*

[b] *College of Chemistry, Chemical Engineering and Biotechnology, Donghua University, Shanghai 201620, People's Republic of China. E-mail: xshi@dhu.edu.cn*

†The authors declare no competing financial interest. A patent related to this work has been registered.[51] Electronic supplementary information (ESI) available: Additional experimental results.

1. M. N. Kim, B. K. Kim and K. H. Han, *J. Gastroenterol.*, 2013, **48**, 681-688.
2. M. F. Yuen, J. L. Hou, A. Chutaputti and P. Asia Pacific Working Party, *J. Gastroenterol. Hepatol.*, 2009, **24**, 346-353.
3. T. R. Ashworth, *Aust. Med. J.*, 1869, **14**, 146-149.
4. G. P. Gupta and J. Massagué, *Cell*, 2006, **127**, 679-695.
5. D. Li and Y. N. Xia, *Adv. Mater.*, 2004, **16**, 1151-1170.
6. G. E. Wnek, M. E. Carr, D. G. Simpson and G. L. Bowlin, *Nano Lett.*, 2003, **3**, 213-216.
7. K. N. Chua, C. Chai, P. C. Lee, Y. N. Tang, S. Ramakrishna, K. W. Leong and H. Q. Mao, *Biomaterials*, 2006, **27**, 6043-6051.
8. S. Agarwal and S. H. Jiang, in *Encyclopedia of Polymeric Nanomaterials*, eds. S. Kobayashi and K. Müllen, Springer-Verlag, Berlin, 2015, pp. 1323-1337.
9. W. J. Li, C. T. Laurencin, E. J. Caterson, R. S. Tuan and F. K. Ko, *J. Biomed. Mater. Res.*, 2002, **60**, 613-621.
10. H. Yoshimoto, Y. M. Shin, H. Terai and J. P. Vacanti, *Biomaterials*, 2003, **24**, 2077-2082.
11. L. Ghasemi-Mobarakeh, M. P. Prabhakaran, M. Morshed, M. H. Nasr-Esfahani and S. Ramakrishna, *Biomaterials*, 2008, **29**, 4532-4539.
12. W. J. Li, R. Tuli, C. Okafor, A. Derfoul, K. G. Danielson, D. J. Hall and R. S. Tuan, *Biomaterials*, 2005, **26**, 599-609.
13. C. Y. Xu, R. Inai, M. Kotaki and S. Ramakrishna, *Tissue Eng.*, 2004, **10**, 1160-1168.
14. Z. Aytac, H. S. Sen, E. Durgun and T. Uyar, *Colloids Surf., B*, 2015, **128**, 331-338.
15. M. F. Canbolat, A. Celebioglu and T. Uyar, *Colloids Surf., B*, 2014, **115**, 15-21.
16. L. Li, G. L. Zhou, Y. Wang, G. Yang, S. Ding and S. B. Zhou, *Biomaterials*, 2015, **37**, 218-229.
17. T. J. Sill and H. A. von Recum, *Biomaterials*, 2008, **29**, 1989-2006.
18. L. Ma, G. Yang, N. Wang, P. C. Zhang, F. Y. Guo, J. X. Meng, F. L. Zhang, Z. J. Hu, S. T. Wang and Y. Zhao, *Adv. Healthcare Mater.*, 2015, **4**, 838-843.
19. L. B. Zhao, Y. T. Lu, F. Q. Li, K. Wu, S. Hou, J. H. Yu, Q. L. Shen, D. X. Wu, M. Song and W. H. OuYang, *Adv. Mater.*, 2013, **25**, 2897-2902.
20. Z. B. Zha, C. Cohn, Z. F. Dai, W. G. Qiu, J. H. Zhang and X. Y. Wu, *Adv. Mater.*, 2011, **23**, 3435-3440.
21. N. G. Zhang, Y. L. Deng, Q. D. Tai, B. Cheng, L. B. Zhao, Q. L. Shen, R. X. He, L. Y. Hong, W. Liu and S. S. Guo, *Adv. Mater.*, 2012, **24**, 2756-2760.
22. S. Hou, L. B. Zhao, Q. L. Shen, J. H. Yu, C. Ng, X. J. Kong, D. X. Wu, M. Song, X. H. Shi and X. C. Xu, *Angew. Chem., Int. Ed.*, 2013, **52**, 3379-3383.
23. S. Hoppmann, Z. Miao, S. L. Liu, H. G. Liu, G. Ren, A. D. Bao and Z. Cheng, *Bioconjugate Chem.*, 2011, **22**, 413-421.
24. L. Y. Feng, Y. Chen, J. S. Ren and X. G. Qu, *Biomaterials*, 2011, **32**, 2930-2937.
25. U. Dharmasiri, S. Balamurugan, A. A. Adams, P. I. Okagbare, A. Obubuafo and S. A. Soper, *Electrophoresis*, 2009, **30**, 3289-3300.
26. Y. Wan, Y. T. Kim, N. Li, S. K. Cho, R. Bachoo, A. D. Ellington and S. M. Iqbal, *Cancer Res.*, 2010, **70**, 9371-9380.
27. J. K. Herr, J. E. Smith, C. D. Medley, D. H. Shangguan and W. H. Tan, *Anal. Chem.*, 2006, **78**, 2918-2924.
28. Y. Y. Wang, L. X. Lü, Z. Q. Feng, Z. D. Xiao and N. P. Huang, *Biomed. Mater.*, 2010, **5**, 054112.
29. P. Miao, J. Yin, L. M. Ning and X. X. Li, *Biosens. Bioelectron.*, 2014, **62**, 97-101.
30. K. Ma, C. K. Chan, S. Liao, W. Y. K. Hwang, Q. Feng and S. Ramakrishna, *Biomaterials*, 2008, **29**, 2096-2103.
31. H. Q. Liu, X. L. Yu, B. Cai, S. J. You, Z. B. He, Q. Q. Huang, L. Rao, S. S. Li, C. Liu and W. W. Sun, *Appl. Phys. Lett.*, 2015, **106**, 093703.
32. Y. L. Zhao, X. Y. Zhu, H. Liu, Y. Luo, S. G. Wang, M. W. Shen, M. F. Zhu and X. Y. Shi, *J. Mater. Chem. B*, 2014, **2**, 7384-7393.
33. M. Elfinger, C. Pfeifer, S. Uezguen, M. M. Golas, B. Sander, C. Maucksch, H. Stark, M. K. Aneja and C. Rudolph, *Biomacromolecules*, 2009, **10**, 2912-2920.
34. A. Jain, L. S. Duvvuri, S. Farah, N. Beyth, A. J. Domb and W. Khan, *Adv. Healthcare Mater.*, 2014, **3**, 1969-1985.
35. X. Fang, H. Ma, S. L. Xiao, M. W. Shen, R. Guo, X. Y. Cao and X. Y. Shi, *J. Mater. Chem.*, 2011, **21**, 4493-4501.
36. X. Fang, S. L. Xiao, M. W. Shen, R. Guo, S. Y. Wang and X. Y. Shi, *New J. Chem.*, 2011, **35**, 360-368.
37. J. C. Li, L. F. Zheng, H. D. Cai, W. J. Sun, M. W. Shen, G. X. Zhang and X. Y. Shi, *Biomaterials*, 2013, **34**, 8382-8392.
38. Y. Hu, J. C. Li, J. Yang, P. Wei, Y. Luo, L. Ding, W. J. Sun, G. X. Zhang, X. Y. Shi and M. W. Shen, *Biomater. Sci.*, 2015, **3**, 721-732.
39. J. C. Li, Y. He, W. J. Sun, Y. Luo, H. D. Cai, Y. Q. Pan, M. W. Shen, J. D. Xia and X. Y. Shi, *Biomaterials*, 2014, **35**, 3666-3677.
40. R. Guo, Y. Yao, G. Cheng, S. H. Wang, Y. Li, M. Shen, Y. Zhang, J. R. Baker, J. Wang and X. Y. Shi, *RSC Adv.*, 2012, **2**, 99-102.
41. S. K. Kamruzzaman, Y. S. Ha, S. J. Kim, Y. Chang, T. J. Kim, L. G. Ho and I. K. Kang, *Biomaterials*, 2007, **28**, 710-716.
42. K. K. Selim, Y. S. Ha, S. J. Kim, Y. Chang, T. J. Kim, G. H. Lee and I. K. Kang, *Biomaterials*, 2007, **28**, 710-716.
43. Y. Y. Cao, Y. He, H. Liu, Y. Luo, M. W. Shen, J. D. Xia and X. Y. Shi, *J. Mater. Chem. B*, 2015, **3**, 286-295.
44. H. Liu, H. Wang, Y. H. Xu, R. Guo, S. H. Wen, Y. P. Huang, W. N. Liu, M. W. Shen, J. L. Zhao, G. X. Zhang and X. Y. Shi, *ACS Appl. Mater. Interfaces*, 2014, **6**, 6944-6953.
45. G. X. Chen, D. Li, J. C. Li, X. Y. Cao, J. H. Wang, X. Y. Shi and R. Guo, *New J. Chem.*, 2015, **39**, 2847-2855.
46. S. KyungáKim, K. MináPark and W. JongáKim, *Chem. Commun.*, 2010, **46**, 692-694.
47. I. K. Park, H. L. Jiang, S. E. Cook, M. H. Cho, S. l. Kim, H. J. Jeong, T. Akaike and C. S. Cho, *Arch. Pharmacal Res.*, 2004, **27**, 1284-1289.
48. Y. Z. Zhang, J. Venugopal, Z. M. Huang, C. T. Lim and S. Ramakrishna, *Polymer*, 2006, **47**, 2911-2917.
49. Y. P. Huang, H. Ma, S. G. Wang, M. W. Shen, R. Guo, X. Y. Cao, M. F. Zhu and X. Y. Shi, *ACS Appl. Mater. Interfaces*, 2012, **4**, 3054-3061.
50. Y. L. Zhao, S. G. Wang, Q. S. Guo, M. W. Shen and X. Y. Shi, *J. Appl. Polym. Sci.*, 2013, **127**, 4825-4832.
51. X. Y. Shi, Y. L. Zhao and Z. Y. Fan, China National invention patent CN104264479A, 2014.

Table 1. Tensile properties of GA vapor-crosslinked PVA/PEI, *m*PEG-PVA/PEI-Ac, and LA-PEG-PVA/PEI-Ac nanofibers (Data are representative of independent experiments and all data are given as mean ± SD, n = 3).

Sample	Breaking strength (MPa)	Failure strain (%)	Young's modulus (MPa)
GA vapor-crosslinked PVA/PEI nanofibers	5.38 ± 0.23	27.94 ± 4.84	84.64 ± 13.50
*m*PEG-PVA/PEI-Ac nanofibers	7.69 ± 0.94	33.37 ± 11.19	197.36 ± 54.93
LA-PEG-PVA/PEI-Ac nanofibers	7.10 ± 0.33	39.60 ± 6.15	112.24 ± 48.11

Figure captions

Scheme 1. Schematic representation of the fabrication of the LA-PEG-PVA/PEI-Ac nanofibers.

Figure 1. ^{1}H NMR spectrum of the LA-PEG-COOH conjugate.

Figure 2. SEM micrograph and fiber diameter distribution histogram of electrospun PVA/PEI (a) and GA vapor-crosslinked PVA/PEI (b) nanofibers.

Figure 3. ATR-FTIR spectra of the PVA/PEI (1), GA vapor-crosslinked PVA/PEI (2), *m*PEG-PVA/PEI-Ac (3), and LA-PEG-PVA/PEI-Ac (4) nanofibers.

Figure 4. SEM micrograph and fiber diameter distribution histogram of the *m*PEG-PVA/PEI-Ac (a) and LA-PEG-PVA/PEI-Ac (b) nanofibers.

Figure 5. Stress–strain curves of GA vapor-crosslinked PVA/PEI, *m*PEG-PVA/PEI-Ac, and LA-PEG-PVA/PEI-Ac nanofibers.

Figure. 6 (a) UV-vis spectra of the HRBC suspensions treated with H_2O, PBS, and *m*PEG-PVA/PEI-Ac or LA-PEG-PVA/PEI-Ac nanofibers at the concentration of 2 mg/mL for 2 h. The inset shows a photograph of HRBCs exposed to water, PBS, and *m*PEG-PVA/PEI-Ac or LA-PEG-PVA/PEI-Ac nanofibers at the concentration of 2 mg/mL, followed by centrifugation. (b) shows the enlarged UV-vis spectra shown in (a) in a wavelength range of 500-600 nm.

Figure. 7 The efficiency of the *m*PEG-PVA/PEI-Ac and LA-PEG-PVA/PEI-Ac nanofibrous mats to capture (a) HepG2 and (b) HeLa cells at different time points.

Figure. 8 Confocal microscopic images of HepG2 cells captured onto (a) *m*PEG-PVA/PEI-Ac and (b) LA-PEG-PVA/PEI-Ac nanofibrous mats at different time points.

Figure. 9 SEM images of HepG2 cells captured onto (a) *m*PEG-PVA/PEI-Ac and (c) LA-PEG-PVA/PEI-Ac nanofibers, respectively, after 240 min culture. (b) High magnification image of (a). (d) High magnification image of (c)

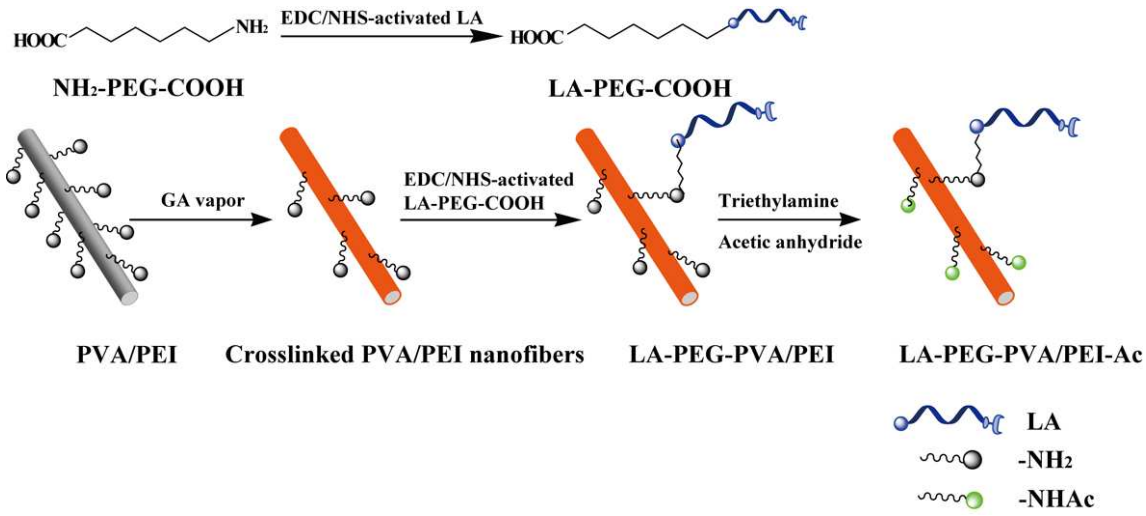

Scheme 1

Zhao *et al.*

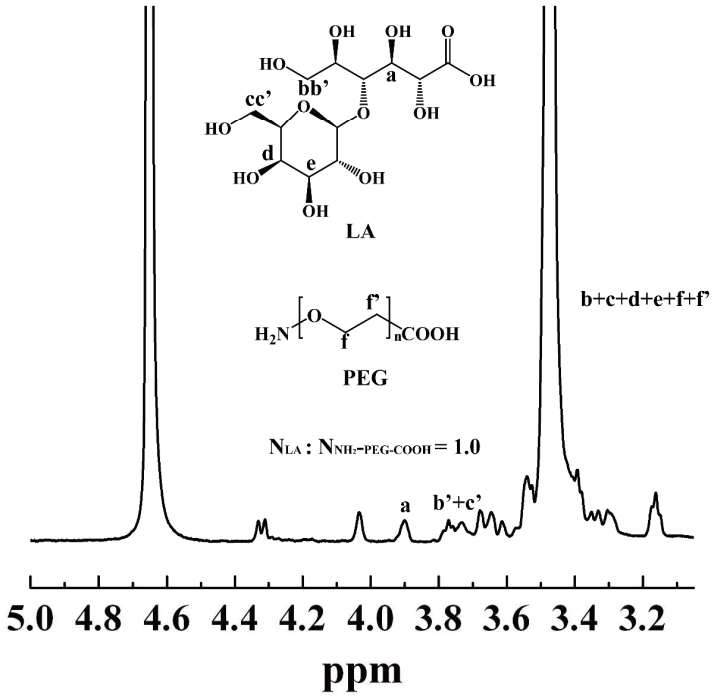

Figure 1

Zhao *et al*.

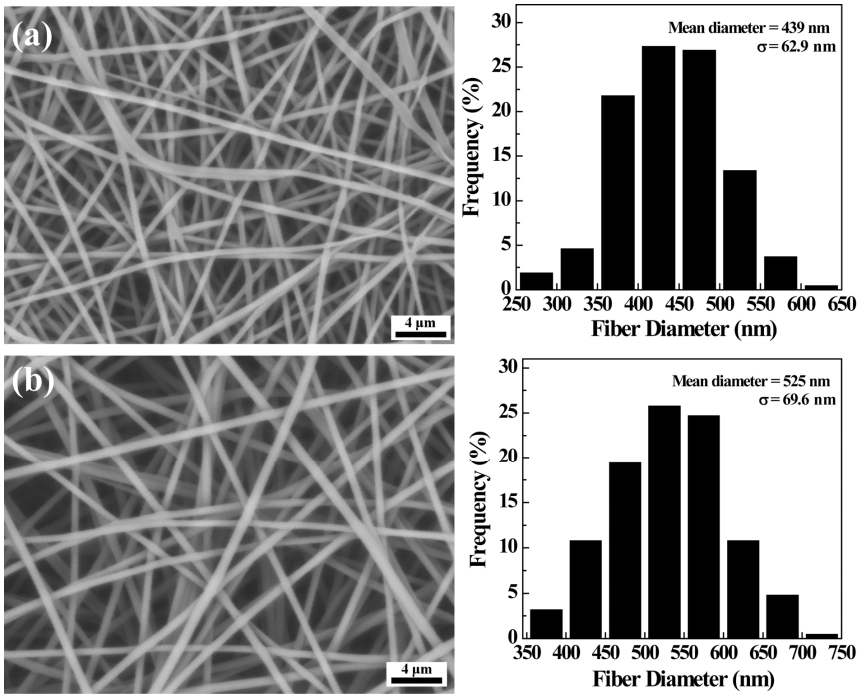

Figure 2

Zhao *et al*.

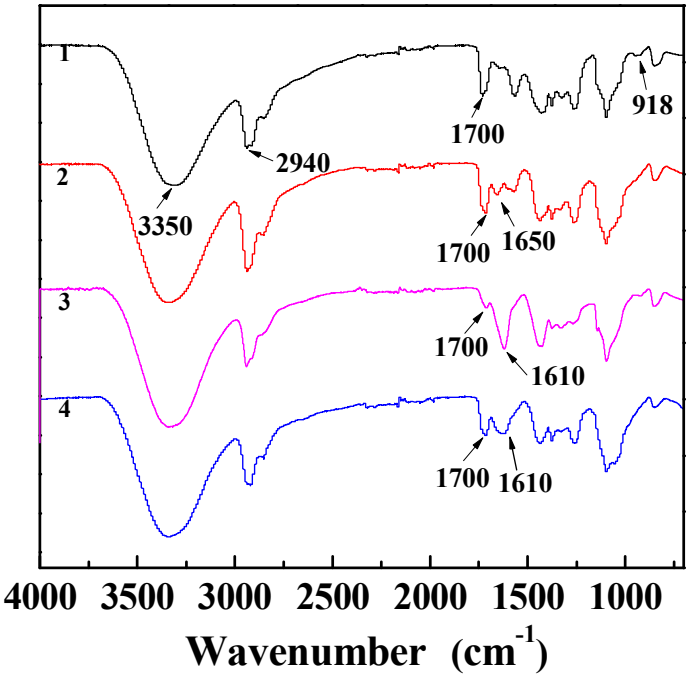

Figure 3

Zhao *et al.*

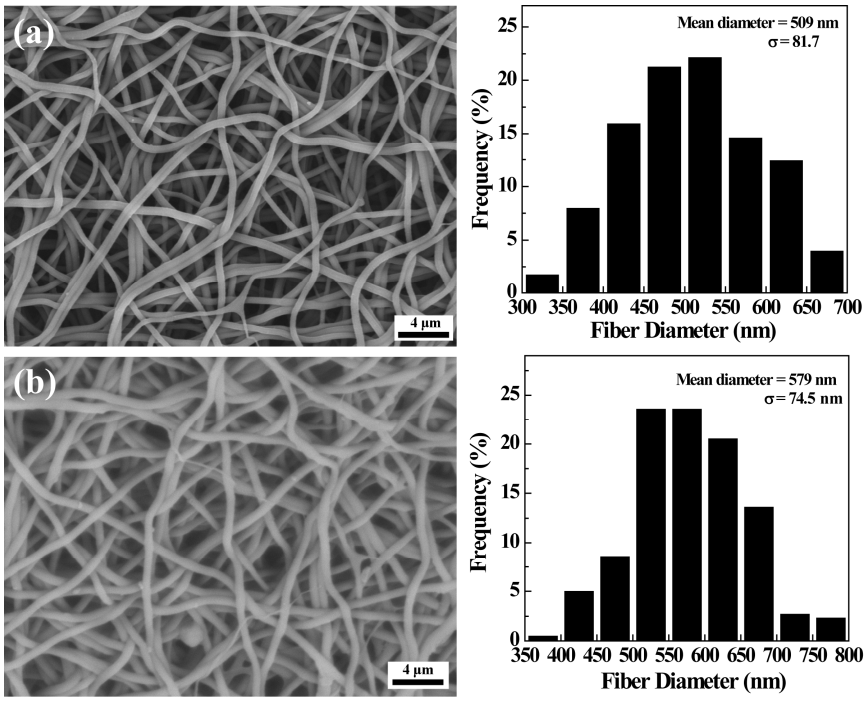

Figure 4

Zhao *et al*.

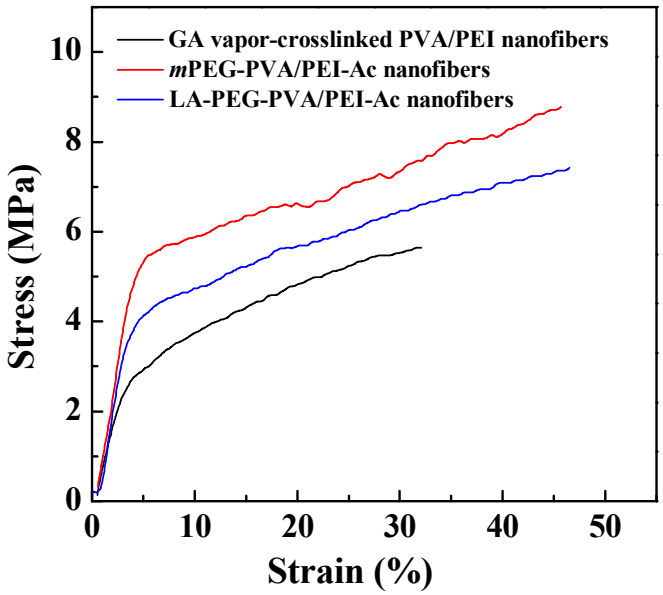

Figure 5

Zhao *et al.*

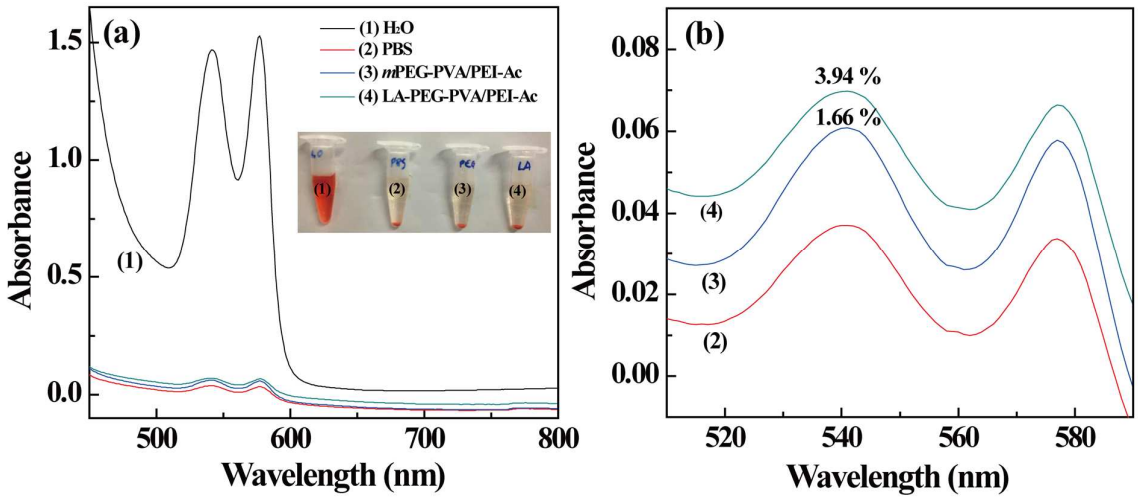

Figure 6

Zhao *et al.*

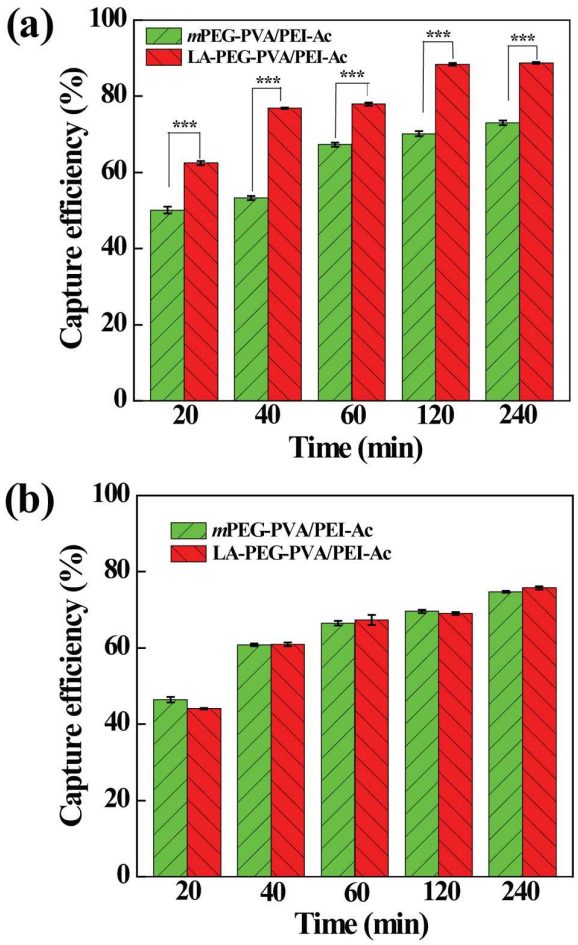

Figure 7

Zhao *et al.*

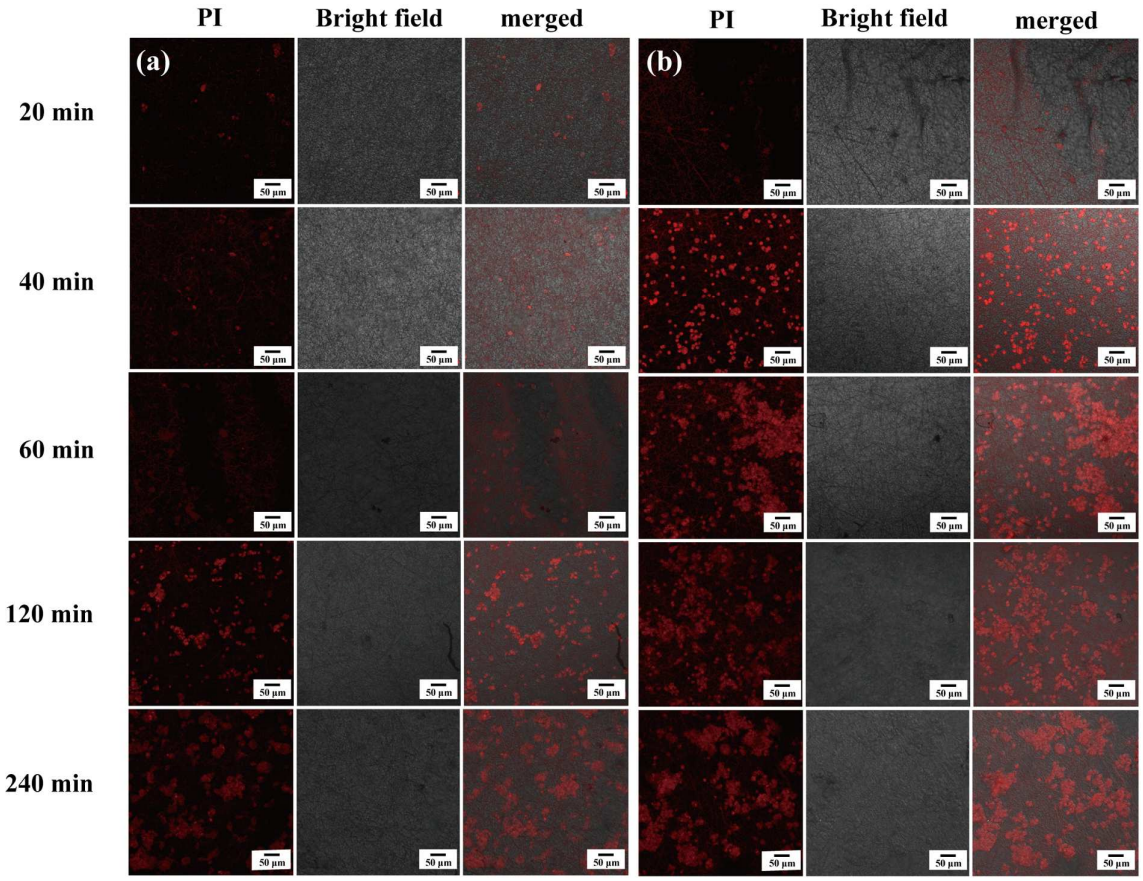

Figure 8

Zhao *et al.*

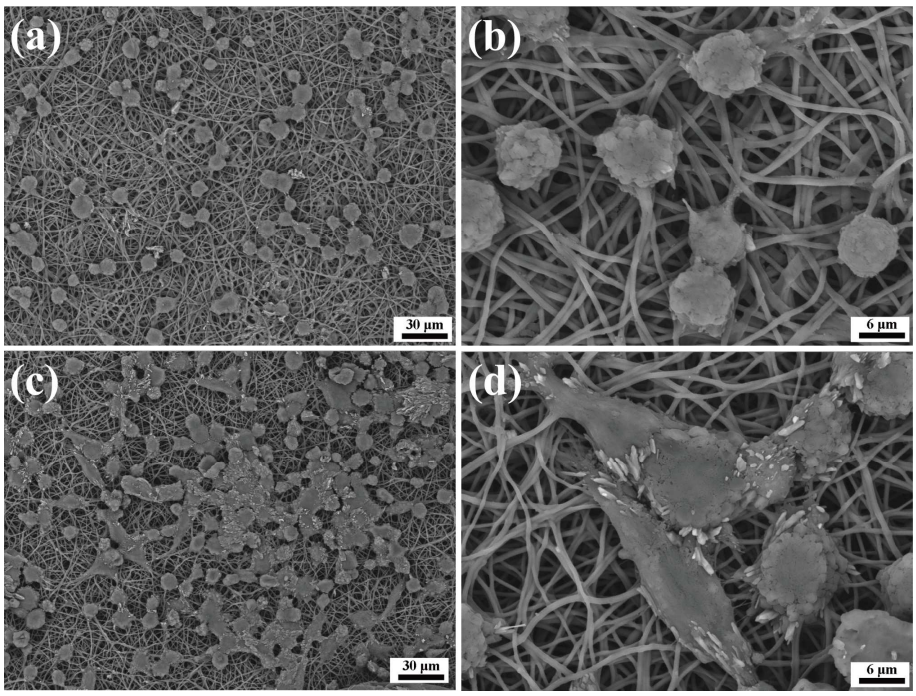

Figure 9

Zhao *et al.*